JOURNAL OF PROPULSION AND POWER
Vol. 24, No. 3, May–June 2008

Matched Pressure Injections into a Supersonic Crossflow Through Diamond-Shaped Orifices

Sadatake Tomioka* and Muneo Izumikawa†
Japan Aerospace Exploration Agency (JAXA),
Kakuda Space Center, Kimigaya, Kakuda, Miyagi 981-1525, Japan
Toshinori Kouchi‡ and Goro Masuya§
Tohoku University,
Aramaki, Aoba, Miyagi 980-8579, Japan
and
Kohshi Hirano¶ and Akiko Matsuo**
Keio University,
Kouhoku, Yokohama, Kanagawa 223-8522, Japan

DOI: 10.2514/1.35177

Matched pressure injections through diamond-shaped injectors were applied to a Mach 2.5 supersonic crossflow, and penetration and mixing characteristics of the injected plume were experimentally investigated. In determining injection conditions, the effective backpressure to the injectant plume was assumed to be equal to pressure on a solid-wedge surface with the identical wedge angle to the injector orifice at a designed flow rate. Both subsonic and supersonic injections were introduced to attain the required low plume pressure at a high supply pressure, ensuring a stable injectant flow rate in reacting flows with high backpressures. The matched pressure injections through the diamond-shaped orifices resulted in little jet-airflow interaction. With the supersonic injection, the plume floated from the injection wall, and the best penetration height was attained, whereas the benefit of matched pressure supersonic injection over the matched pressure sonic injection was not as remarkable as the circular injector case. The penetration height increased at an overexpanded condition, while the maximum mass fraction decay was insensitive to the injection pressure. In the case with the subsonic injection, the plume shape was similar to a pillar, and a certain fraction of the injectant was left within the boundary layer region. The penetration height as well as the maximum mass fraction decay was found to be insensitive to the injection pressure.

Nomenclature

A	=	cross-sectional area
C_d	=	discharge coefficient
D, D_{eff}	=	diameter, effective diameter, Eq. (1)
G	=	fuel mass flow rate
H	=	penetration height
J	=	jet-to-freestream dynamic pressure ratio
M	=	Mach number
p, P	=	static pressure, total pressure
R_b	=	effective radius, Eq. (2)
V	=	velocity
X, Y	=	streamwise location, and spanwise location from injector center
Z	=	height from injection wall
γ	=	specific heat ratio
ρ	=	density

Subscripts

a	=	freestream
j	=	jet, plume
m	=	measured within additional plenum
p	=	measured with in-stream probe
112, 347	=	probing stations at $X = 112$ mm, and $X = 347$ mm

I. Introduction

THE supersonic combustion ramjet (scramjet) operation, including dual-mode operation, is a vital part of rocket-based combined-cycle engines, as the operation in a wide flight speed range through ascent trajectory to low-Earth orbit is a key factor to reduce the onboard oxygen consumption and to increase specific impulse. As the flow speed after the compression process remains supersonic, the residence time within the combustor will only be of the order of milliseconds. Thus, efficient fuel jet penetration and air/fuel mixing must be achieved within the short duration, and many studies on penetration augmentation devices have been carried out. Northam et al. [1] proposed a so-called ramp injector to introduce streamwise vortices to enhance the penetration and the mixing. This configuration was proven to efficiently increase the penetration height; however, the inevitable intrusive-device/airflow interaction caused excess total pressure loss, drag, and thermal load on the device. Thus, flush-mounted fuel injection from the combustor wall is an attractive arrangement if sufficient penetration is achievable.

Various noncircular injection orifice shapes have been tested in attempts to attain better penetration and mixing capabilities. Barber et al. [2] introduced a wedge-shaped orifice having a wedge-shaped front half and a round-shaped back half. By avoiding the occurrence

Presented as Paper 5402 at the 43rd Joint Propulsion Conference and Exhibit, Cincinnati, Ohio, 8–11 July 2007; received 17 October 2007; accepted for publication 4 February 2008.

*Senior Researcher, Advanced Technology Research Group, Institute of Space Transportation. Member AIAA.
†Researcher, Combined Propulsion Research Group, Institute of Space Transportation. Member AIAA.
‡Assistant Professor, Department of Aeronautical Engineering. Member AIAA.
§Professor, Department of Aeronautical Engineering. Member AIAA.
¶Graduate School Student, Department of Mechanical Engineering. Student Member AIAA.
**Associate Professor, Department of Mechanical Engineering. Member AIAA.

of boundary layer separation ahead of the injectant jet, the wedge-shaped injection resulted in a better penetration than the conventional circular injector. However, the round-shaped back half caused a separation in the wake of the jet, and the low-pressure condition within the separation region caused intensive disturbances. Tomioka et al. [3] proposed a diamond-shaped orifice to further reduce plume/airflow interaction and to further increase plume penetration height. At a low jet-to-freestream dynamic pressure ratio, this orifice showed good penetration compared to the conventional circular orifice and the wedged-shaped orifice. At a high dynamic pressure ratio, on the other hand, the plume experienced an axis switching to collapse the effectiveness of the orifice shape, and the resulting penetration height was comparable to that of the circular injector.

At the low injection pressure condition, the injection pressure was so selected that the static pressure of the plume is equal to that of the airflow after passing through an oblique shock wave by a "solid wedge" representing the plume shape (termed as the matched pressure injection). The advantage of the matched pressure, supersonic injection over the underexpanded sonic injection was shown for the circular orifice case [4]. Thus, introducing the matched pressure supersonic injection to the diamond-shaped orifice case might show some benefits. However, recent studies on the diamond-shaped injector [3,5,6] were for sonic injection, and no publication is available on the supersonic injection through the diamond-shaped orifices.

The supersonic injection may have another benefit in the real hypersonic engines. Occurrence of combustion within supersonic flows increases the pressure level within the combustor by an order of 5, and this drastic change can deteriorate the matched pressure condition, and even the choking condition across the injector orifice. With the supersonic injection, the choking condition will be sustained even with the drastic increase in the airflow pressure, as injection pressure will be quite high against the combustor pressure level. In this sense, having smaller orifices at the entrance of the larger injector's plenum will also work to sustain the fuel flow rate, while the jet through the orifices will be decelerated to subsonic speed within the plenum and will issue out into the supersonic flow.

In the present study, the above-mentioned two different schemes to attain the matched pressure injection were introduced, one with the supersonic injection and another with the subsonic injection, the latter designed for about a sonic speed injection in the absence of the high backpressure due to combustion. Characteristics of these two injection schemes were experimentally investigated with gaseous helium injection into a Mach 2.5 supersonic crossflow. First, the flowfields with these new matched pressure injections through the diamond-shaped orifices were compared to those with the sonic, underexpanded injection through the diamond-shaped orifice to identify the benefits of the matched pressure injection. Next, characteristics of these matched pressure injections through the diamond-shaped orifices, namely, penetration height and injectant maximum concentration, were measured and compared to those with the conventional sonic, underexpanded injection through a circular orifice to quantify the benefits of these new injection schemes. The characteristics at off-design injection pressures were also investigated to evaluate their changes in the combusting flowfield.

II. Experimental Apparatus and Measurements

A. Experimental Apparatus

A Mach 2.5 wind-tunnel facility at the Japan Aerospace Exploration Agency—Kakuda Space Center was used in the present study. Figure 1 shows a schematic of the arrangement and the shape of the orifices. The facility is a blowdown-type wind tunnel with a Mach 2.5 nozzle, with its outlet area being 94.3 mm in width and 51 mm in height. The tunnel average plenum conditions were 750 kPa (P_a) and room temperature, which resulted in a freestream unit Reynolds number of 4.4×10^7/m. The X, Y, and Z coordinates were in the streamwise direction, the spanwise direction, and the vertical direction, respectively, with a right-hand system and with the origin at the center of injector orifices. The 99% velocity and

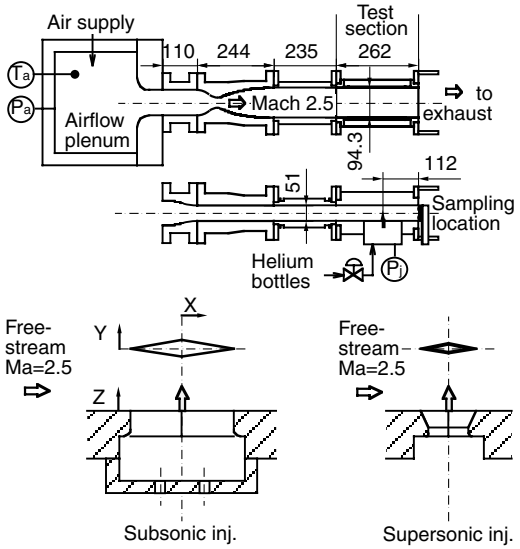

Fig. 1 Schematic diagram of facility and injectors.

displacement thicknesses of the incoming boundary layer at the entrance of the test section were 18.5 and 5.1 mm, respectively.

Room temperature helium was used as the injectant in the present study to simulate hydrogen injection. The injectant supply pressure was regulated with a pressure regulator valve, and the flow rate was regulated via a choking condition through a needle valve located downstream of the pressure regulator valve.

B. Measurement and Data Reduction

Both the airflow plenum pressure (P_a) and the injection pressure (P_j) were monitored with pressure transducers. The injectant flow rate was measured with a sharpened-edge orifice flow meter with an error of $\pm 1\%$, to estimate the orifice discharge coefficient and the effective radius to be addressed next.

Surface flow patterns near the injector were visualized with an oil flow technique.

Gas sampling was carried out at several streamwise locations, and plume penetration was evaluated. In the present study, the location with maximum injectant fraction was defined as the center of the plume, and its height from the injection wall was defined as the penetration height. The gas sampling was carried out in a 2 mm interval in the height (Z) direction on the plane through the plume symmetry, so that a reading error of ± 1 mm for the penetration height was expected. The measurement error in the maximum injectant fraction including repeatability was $\pm 3\%$ in the volume fraction, and $\pm 3\%$ in the deduced mass fraction. To attain an injectant fraction contour, a scarce interval of 4 mm in the height direction was used with a spanwise interval of 5 mm.

Penetration heights were usually normalized with the effective diameter (D_{eff}) defined as

$$D_{\text{eff}} = (4A_j/\pi C_d)^{1/2} \tag{1}$$

where A_j is the injector orifice area and C_d is the discharge coefficient. Injection at different injection pressures through an identical orifice results in a different injectant flow rate. In engine designs, the limiting factor is total fuel flow rate, so that one would use a larger injector for lower injection pressure to attain an identical injectant flow rate. Thus, normalization with an identical geometrical scale such as the effective diameter can result in an under-/overestimation of the plume penetration height for a reduced-/increased-injection pressure from the design value. For example, when the injection pressure is reduced to half, the area of the orifice should be doubled; that is, the effective diameter should be increased by 40%, and also the penetration height should be increased by 40%. Thus, we should normalize both of the height and the streamwise distance from the injector with a length scale in which injectant flow

rates are taken into account, to compare the results with different injection pressure. Barber et al. [2] introduced the effective radius defined in [7] to summarize the penetration data for various injector orifice shapes. The effective radius (R_b) is defined as [7]

$$R_b = (G_j/\rho_a V_a)^{1/2} \tag{2}$$

where G_j is the injectant mass flow rate. This length scale was originally introduced to summarize aerodynamic effects of injection on interaction with freestream, injectant being through various-size orifices at various injection pressures [7], and the injectant flow rate was found to be the governing parameter. By using the effective radius, a reduced flow rate to half of the design value results in a reduced length scale to $1/\sqrt{2}$, so that the normalized penetration height with the effective radius reflects the above-mentioned necessary change in the orifice size. In the present study, both the penetration height and the streamwise distance between the center of the injector and the probing location (X) were normalized with R_b to discuss the effects of the injector geometry and injection conditions on the penetration height growth and the maximum mass fraction decay. Note that this normalization was necessary 1) to compare the data with the diamond-shaped orifices with different sizes, and 2) to compare the data to those with the circular injector with different effective diameters and different injection pressures. In the present setup, measurement errors on the freestream states and the injectant mass flow rate resulted in $\pm 2\%$ estimation error of the effective radius.

C. Injector Design and Injection Conditions

To design the injector shape for matched pressure conditions, it was necessary to estimate the effective backpressure to the plume, which is in turn a function of the plume shape. Billig et al. [8] evaluated the effective backpressure to the circular plume issued into supersonic crossflow as two-thirds of the freestream pitot pressure, approximating average pressure on the upwind side surface of a cylinder. In the case with the plume through either the diamond-shaped injector or the wedge-shaped injector, the flowfield was expected to be simpler because of the less intensive interaction between the plume and the airflow as shown in [3]. In the present study, as in the previous study [3], the effective backpressure (p_{eb}) was evaluated as the static pressure of the $M2.5$ airflow after passing through an oblique shock wave caused by a solid wedge with identical half-angle to the diamond-shaped orifice (10 deg throughout the present study), that is, $p_{\mathrm{eb}} = 0.109 \times P_a$. The "matched pressure injection" was defined as the case where the plume static pressure at the exit of the injector orifice was identical to the effective backpressure.

In the present study, two sonic injectors, two supersonic injectors, and one subsonic injector were used. In all cases, injection was perpendicular to the freestream to use as much plume momentum as possible for penetration. The large sonic injector was 32.7 mm in length and 5.8 mm in width, designed for matched pressure sonic injection at a jet-to-freestream dynamic pressure ratio of 0.36. The small sonic injector was 12.7 mm in length and 2.2 mm in width, and was used for underexpanded sonic injection at the dynamic pressure ratio of 2.4, with the injectant flow rate being almost identical to that through the large sonic injector at the matched pressure condition. At this high dynamic pressure ratio, the diamond-shaped orifice was reported to lose its effectiveness [3], and the penetration height was almost identical to that of the plume through a circular orifice at the same area and flow rate.

The small supersonic injector had identical throat dimensions to the small sonic injector, and had a diverging section to accelerate the plume to Mach 2.4 (in the case with helium) with the diverging half-angles of 5 and 25 deg in the short and long axis directions, respectively. The medium supersonic injector had a twice as large throat area as the small injector, and the plume was accelerated to Mach 1.9 with identical diverging half-angles. However, this injector was designed for hydrogen injection, so that the nozzle was in a slightly overexpanded condition at the design flow rate as will be shown later.

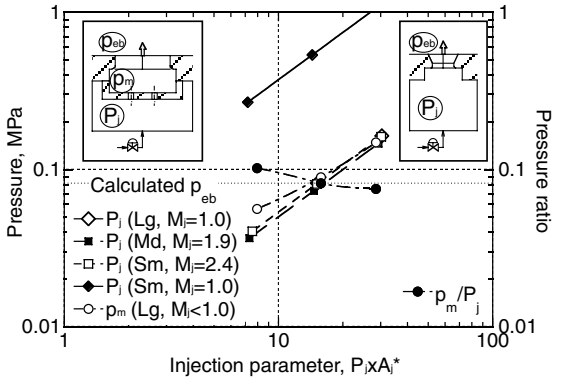

Fig. 2 Relation between supply pressure and additional manifold pressure.

An additional small plenum was attached to the large sonic injector, and small circular "supply" orifices with identical throat areas to the small sonic injector were placed at the entrance of the plenum. A choking condition at this supply orifice was ensured throughout the present study. At the design flow rate, the large diamond-shaped orifice was expected to choke against the effective backpressure, although it would not against an elevated backpressure in a reactive flow case. This injector was termed a "subsonic" injector in the present study.

Figure 2 shows the calculated variations of the plume static pressure at the exit of the orifices against an injection parameter, that is, supply pressure (P_j) $\times$ throat area (A_j^*), which denotes the injectant flow rate. Note that the injectant flow rate at the design condition for different injector orifices was set to be identical in the present study, so that the probing measurements with different injection orifice sizes at a streamwise location (X) could be fairly compared as they were at an identical X/Rb. For the case with the subsonic injector, pressure within the additional plenum (p_m) was monitored and its variation is shown in the figure, as the calculation of the pressure loss of the plume in a limited length was difficult.

At the design point, the supply pressure for the injectant flow rate was fixed to be about 14.5 g/s ($P_j \times A_j^* = 15$ N at room temperature of 288 K). At this flow rate, the matched pressure condition was expected for the large sonic injector and the small supersonic injector. The medium supersonic injector should be at a 20% overexpanded condition ($p_j = 0.8 \times p_{\mathrm{eb}}$). For evaluation of off-design characteristics, the flow rate was either reduced to half or doubled by changing the supply pressure.

At the design flow rate, the injection pressure and the plume static pressure should be 170 and 82 kPa, respectively, with the large sonic diamond-shaped orifice being choked. With the additional plenum, however, the choking condition at the diamond-shaped orifice was not attained at the design point, as p_m/P_j did not reach a constant value, whereas the value (ratio over the supply orifice) ensured the choking condition at the supply orifice. The additional plenum pressure (p_m) was 89 kPa at the design point, rather close to the effective backpressure. The additional plenum length was not adequate to have the jets through the supply orifices to fully expand to the diamond-shaped orifice as will be shown in Fig. 3, so that there should be an aerodynamic connection between the near field to the injector orifice and the additional plenum. As shown in the figure, a higher flow rate resulted in a constant value of p_m/P_j, showing that the choking condition was attained.

III. Results and Discussions

A. On-Design Characteristics

In this section, characteristics of the plume through both supersonic and subsonic injectors were compared to those of the underexpanded sonic injector at an almost identical injectant flow rate around the design value. The penetration characteristics were

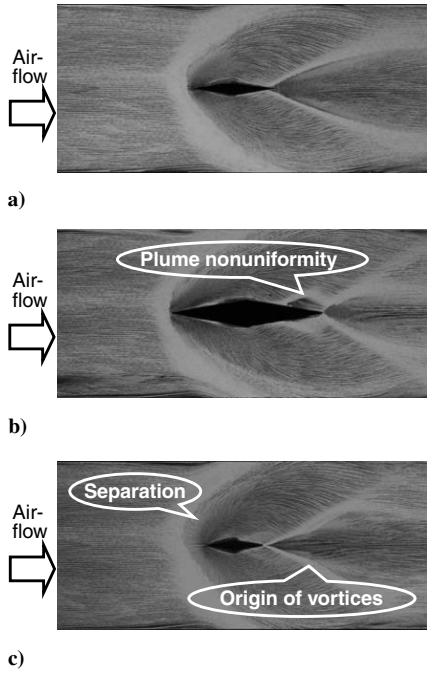

Fig. 3 Oil flow patterns around a) small supersonic injector, b) large subsonic injector, and c) small sonic injector.

also compared to those of the sonic plume through a circular injector at the matched pressure condition, that is, the jet static pressure being two-thirds of the pitot pressure of the airflow (dynamic pressure ratio of 1.1 under the present conditions). The orifice throat area (diameter of 6 mm) of the circular injector was equal to that of the medium supersonic injector, and the flow rate was almost identical to the design value for the diamond-shaped injectors. Details of the circular injector and results will be found in [9]. Note that only the circular injector cases were specifically noted in the present study.

Figure 3 shows the oil flow patterns with 1) the small supersonic injector, 2) the large subsonic injector, and 3) the small sonic injector, respectively. In the figures, the airflow is from left to right. In the case with the sonic injection, the plume expanded rapidly in the spanwise direction to cause so-called axis switching, collapsing the effectiveness of the plume. Thus, the plume became a blunt obstacle to the airflow similar to the circular plume, and separation ahead of the plume was formed. This separation and resulting higher effective backpressure suppressed the growth of the plume height. The complicated flow pattern in the wake shows some traces of streamwise vortices. In the case with the supersonic injection, there remained a slight separation ahead of the plume, as the diverging section of the injector was not well contoured to attain uniform static pressure at its exit, and axis switching at a lesser degree might take place. However, trace of the streamwise vortices is not obvious in this case. In the case with the subsonic injector, the plume was expected to be at almost matched pressure condition, and little separation ahead of the plume and little trace of streamwise vortices were observed. The disturbance to the airflow in the vicinity of the rear half of the large orifice was due to nonuniformity in the injectant flow within the orifice, as the supply orifices are located too close to the diamond-shaped orifice to attain enough spread of the jet within the cross section of the diamond-shaped orifice. However, as will be shown in Figs. 6, this nonuniformity had little effect on the plume penetration.

Figure 4 shows the injectant contours with 1) the small supersonic injector, 2) the large subsonic injector, and 3) the small sonic injector, respectively, at $X = 112$ mm. The underexpanded plume from the small sonic injector shows a similar contour to the underexpanded plume from circular orifices [3], a mushroom-like shape dominated by the streamwise vortices. The matched pressure plume from the small supersonic injector shows quite a different shape, a ball-like shape floating above the injection wall. Deformation of its shape due

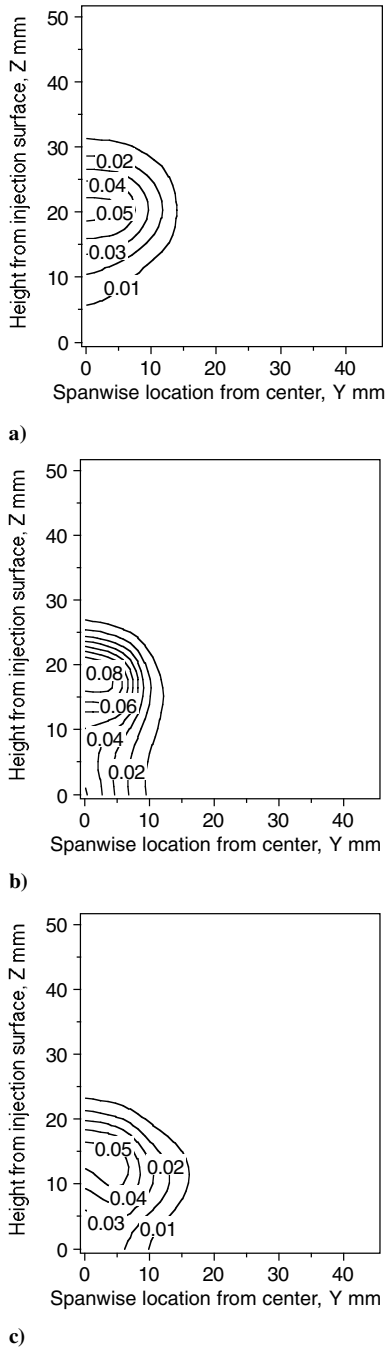

Fig. 4 Injectant mass fraction contour at $X = 112$ mm with a) small supersonic injector, b) large subsonic injector, and c) small sonic injector

to streamwise vortices was not observed as the smooth flow near the wall around the injector caused less intensive streamwise vortices compared to the sonic injection case. Even without the help of streamwise vortices, the plume penetrated farther into the airflow than the underexpanded sonic plume. The matched pressure plume from the large subsonic injector shows a different shape to the matched pressure supersonic plume, a pillar-like shape with a high injectant concentration region both on top (termed as plume core) and near the wall. Again, deformation of its shape due to streamwise vortices was not observed, as the smooth flow near the injector wall suppressed the generation of streamwise vortices.

In both matched pressure injection cases, the penetration height was slightly larger with the supersonic injection, though the supply pressure to the injector was almost identical, and both injections were associated with little separation ahead of the plume and little traces of streamwise vortices in the wake. In the subsonic injection case, a

high-pressure jet through the small supply orifices issued into the additional plenum in an underexpanded jet and decelerated to subsonic speed through a shock-wave system. This deceleration was associated with a sizable total pressure loss of the plume, resulting in a smaller penetration height than that with the supersonic injections.

The lack of streamwise vortices generation might retard the growth of the penetration height for the matched pressure injection cases, so that the gas sampling was also carried out at a farther downstream location ($X = 347$ mm). Figures 5a and 5b show the injectant mass fraction distributions in the X–Z symmetry plane at $X = 112$ mm, and those at $X = 347$ mm, respectively. In these figures, data with the small sonic injector, the small supersonic injector, the medium supersonic injector, the large subsonic injector, and the large sonic injector (the supply orifices being removed) are shown. Though a little bit higher injectant fraction near the injection wall was observed with the large sonic injector case, the distribution around the maximum fraction was almost identical to that with the large subsonic injector at both locations, showing that the plume conditions were almost identical at the exit of the diamond-shaped orifice. Furthermore, the injectant distributions near the wall were also similar in tendency, that is, a certain fraction of injectant is being left within the boundary layer with increasing value toward the injection wall. This tendency was not observed in the cases with the sonic underexpanded injection nor the supersonic matched pressure injections. Thus, this tendency was not characteristic of the matched pressure injection condition. For the supersonic injection cases, a higher injection Mach number resulted in a larger penetration height, a lower injectant mass fraction toward the injection wall, and a less steep mass fraction gradient toward the freestream.

The penetration height and the maximum injectant mass fraction were determined from Figs. 5 and were summarized in Figs. 6 together with those with the circular matched pressure injection, in which the length scales were normalized with the effective radius [Eq. (2)]. In Fig. 6a, data with the small supersonic injector and the large subsonic injector were compared to those with the small underexpanded sonic injector and the matched pressure circular injector. At near field to the injector location ($X/R_b = 10 \sim 25$), the

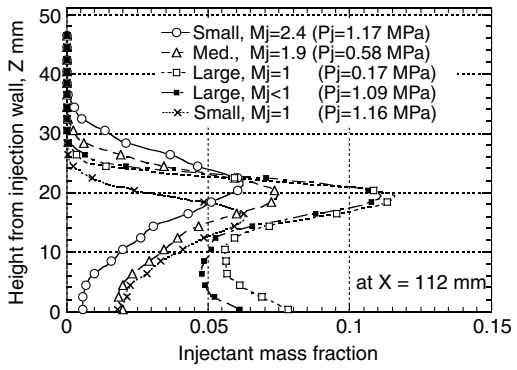

a)

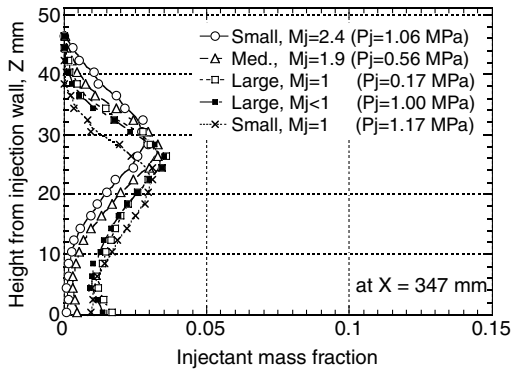

b)

Fig. 5 Injectant mass fraction distributions with various injectors.

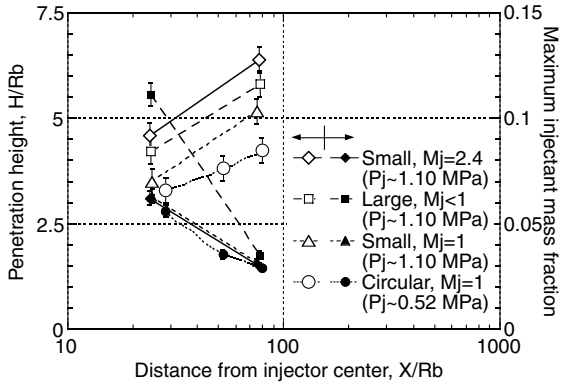

a)

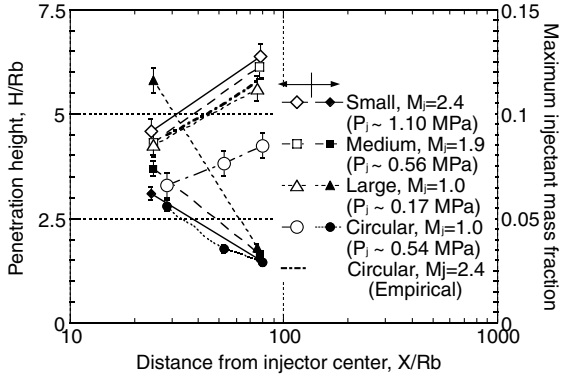

b)

Fig. 6 Summary of penetration and mixing with a) various injectors and b) various injection Mach numbers.

matched pressure circular injection resulted in an equal or larger penetration height to the underexpanded diamond-shaped injection, which was consistent to the previous results [3]. However, the growth of the penetration height was larger with the underexpanded diamond-shaped injection due to a more intensive interaction between the freestream and the plume resulting in more intensive streamwise vortices. Note that the maximum fraction was almost identical in both injection cases.

The plume through the small supersonic injector had 32 and 24% larger penetration heights than that through the small sonic (underexpanded) injector at $X = 112$ and 347 mm, respectively, whereas the maximum fraction was almost identical. The plume through the large subsonic injector also had 21 and 13% larger penetration heights than that through the small sonic injector at $X = 112$ and 347 mm, respectively. The maximum fraction, however, was about 80% larger than those with other injectors at $X = 112$ mm, showing that this injector had poor mixing capability, especially in the near field. The maximum fraction with this injector decreased rapidly, and only 10% larger than those with other injectors at $X = 347$ mm. Although the matched pressure injections resulted in larger initial penetration heights, they resulted in smaller growth ratios (H_{347}/H_{112}) than the underexpanded injections, as the latter injections were associated with more intensive streamwise vortices. However, the penetration heights with the matched pressure injections were still larger than those with the underexpanded diamond-shaped and circular injections at far field ($X/R_b = 70$–80), showing that the penalty of the less intensive streamwise vortices generation on the penetration height growth was not definitive in the present conditions.

In Fig. 6a, the supersonic injection resulted in a larger penetration height than the subsonic injection for the matched pressure injection. Thus, the effects of the injection Mach number were examined. Figure 6b shows the penetration height and the maximum injectant mass fraction, with the large sonic injector ($M_j = 1.0$), the medium supersonic injector ($M_j = 1.9$), and the small supersonic injector

($M_j = 2.4$). Note that all three cases were at the matched pressure injection condition, with a slight deviation for the medium injector case. With the increase in the plume Mach number, the penetration height slightly increased, and the maximum injectant mass fraction decreased substantially. Schetz and Billig [10] made a parametric estimation on the effects of the injection Mach number on the penetration height of the matched pressure circular plume, and Orth and Funk [11] experimentally confirmed the validity of that estimation. The resulting estimation for the matched pressure injections at identical flow rate is given as

$$H_{M>1}/H_{M=1} = (J_{M>1}/J_{M=1})^{0.4} \times (d_{M>1}/d_{M=1})^{0.6} = \left\{[(\gamma+1)/2]/\left[1+(\gamma-1)/2\times M_j^2\right]\right\}^{0.15} \times M_j^{0.5} \quad (3)$$

in which $M > 1$ and $M = 1$ denote supersonic and sonic injection, respectively, both at the matched pressure condition. The estimated penetration height with the supersonic circular injection at $M_j = 2.4$ is shown in the figure with a dashed line, showing that supersonic injection was more beneficial for the circular injector than for the diamond-shaped injector. However, the penetration height with the latter injector was still superior to that with the former injector, showing the effectiveness of the diamond-shaped supersonic injection in the present conditions.

B. Off-Design Characteristics

In this section, the injectant flow rate was reduced to half or doubled from the design value for the matched pressure injections, to investigate off-design characteristics of the supersonic and subsonic injections. For the supersonic injection, the small injector was used, and those results are described first.

Figure 7a shows the injectant mass fraction distributions in the X–Z symmetry plane at $X = 112$ mm. The penetration height increased with the injection pressure. However, increase in the penetration height was 16% for the doubled injection pressure, that is, for the doubled jet-to-freestream dynamic pressure ratio. In the case with the circular injector, the penetration height (defined as the Mach disk height) is reported to be proportional to the square root of the dynamic pressure ratio [4], so that the doubled dynamic pressure ratio should increase the penetration height by about 40%. In [9], the plume penetration data with gas sampling were correlated with the jet-to-freestream effective velocity ratio and the orifice diameter, and the correlation implies about 30% enhancement in the penetration height defined as the plume core height, by doubling the dynamic pressure ratio. The measured increase in the penetration height was lower than that with either prediction. Figure 7b shows the injectant mass fraction distributions in the X–Z symmetry plane at $X = 347$ mm. The penetration height still increased with the injection pressure, and the doubled injection pressure resulted in a 22% larger penetration height at this far downstream location. At both locations, the maximum fraction increased with the injection pressure, but the proportionality was rather poor.

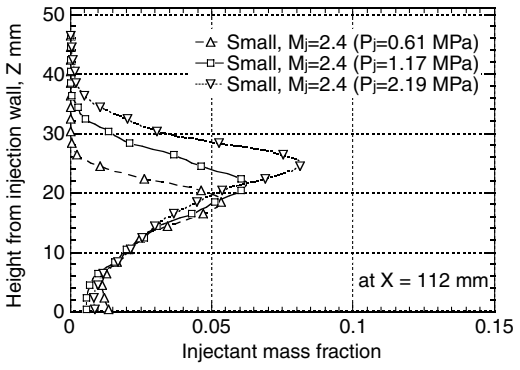

a)

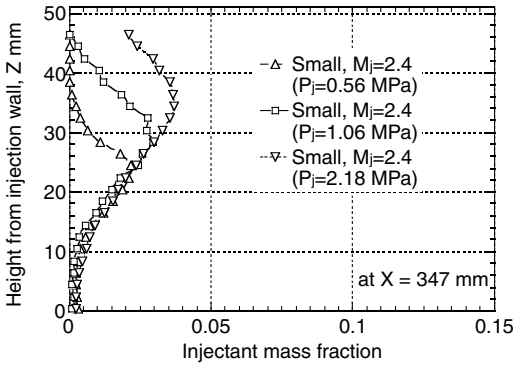

b)

Fig. 7 Injectant mass fraction distributions with large supersonic injectors.

As described before, it was more reasonable to scale the length with a characteristic length taking the injectant flow rate into account, that is, the effective radius, to compare the data with various injectant flow rates. Both the distance between the center of the injector and the measurement location and the penetration height were normalized with the effective radius, and the scaled-penetration height as well as the maximum injectant mass fraction is shown in Fig. 8. For reference, those with the circular sonic injections at the matched pressure condition, at a reduced injection pressure to half, and at a doubled injection pressure, are also shown in the figure, which shows an increased scaled-penetration height and a larger growth with the injection pressure. As a result, the scaled-penetration heights for various injection pressures with the circular injector were almost identical in the near field to the injector, which is consistent with the previous result [4] showing that the initial penetration height is proportional to the orifice diameter and square root of the dynamic pressure ratio (and thus, the square root of the injection pressure). In other words, the matched pressure injection ($P_j \sim 0.5$ MPa) did not act favorably for penetration enhancement in the case with the circular injector. Pressure distribution around the circular plume varied from place to place, so that the shock-wave generation due to the local mismatch in the static pressure might reduce the jet total pressure even at the matched pressure condition.

Contrary to the circular injection case, a lower injection pressure resulted in a larger scaled-penetration height with the diamond-shaped supersonic injection. The growth ratio ($\{H/R_b\}_{347}/\{H/R_b\}_{112}$) was almost insensitive to the injection pressure, while the growth rate ($\Delta\{H/R_b\}/\Delta\{X/R_b\}$) slightly increased with the injection pressure. The decay of the maximum fraction was insensitive to the injection pressure, with these variations being very close to those with the circular, sonic injections.

When the injection pressure was over the design value, the plume became underexpanded, so that the axis switching might retard the effectiveness of the plume shape. When the injection pressure was under the design value, the plume became overexpanded, and thus, selectively shrunk in the width direction contrary to the axis switching for the underexpanded case, so that the plume might

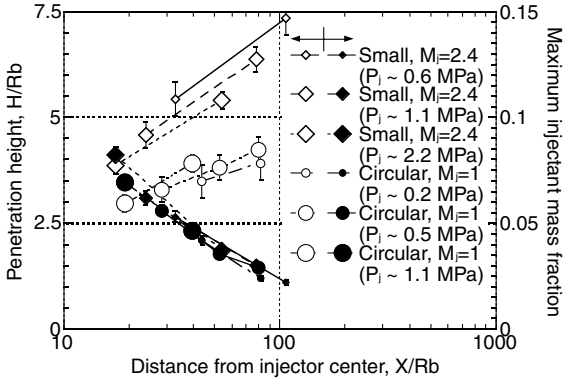

Fig. 8 Summary of penetration and mixing with supersonic injection at various injection pressure.

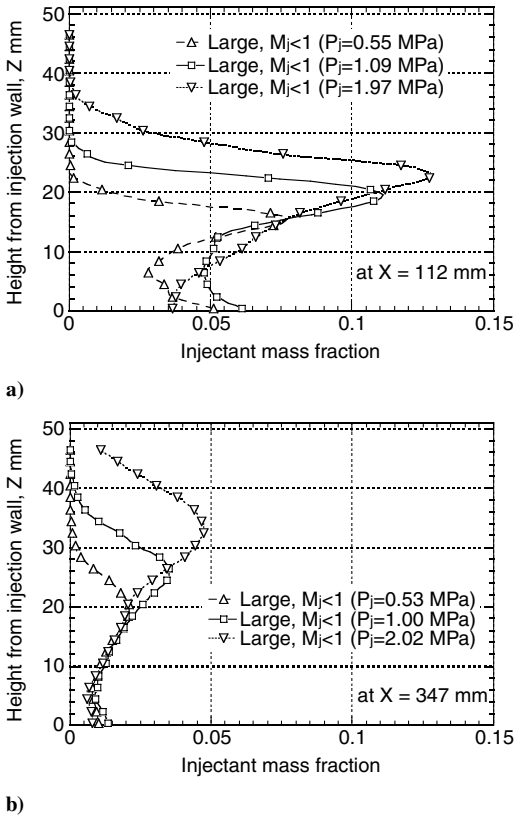

Fig. 9 Injectant mass fraction distributions with large subsonic injectors.

become sharper with a reduced interaction with the airflow, resulting in the increased penetration height. This characteristic may be beneficial for applying this injection scheme to the combustor, as the increase in the backpressure due to combustion will bring the injection condition to be overexpanded, thus increasing the penetration height.

Off-design characteristics of the subsonic injector are described next. Figure 9a shows the injectant mass fraction distributions in the X–Z symmetry plane at $X = 112$ mm. Both the penetration height and the maximum fraction increased with the injection pressure. Again, the penetration height was not proportional to the square root of the injection pressure. The higher injection pressure resulted in a larger total pressure loss of the jet within the additional plenum, so that the penetration was less enhanced with injection pressure than expected. Figure 9b shows the injectant mass fraction distributions in the X–Z symmetry plane at $X = 347$ mm. The penetration height still increased with the injection pressure, with its sensitivity being more apparent at this streamwise location. To compare the data with various injectant flow rates, both the distance between the center of the injector and the measurement location and the penetration height were normalized with the effective radius, and the scaled-penetration height as well as the maximum injectant mass fraction is shown in Fig. 10. With this injection scheme, the scaled-penetration height was insensitive to the injection pressure, as the injection pressure was somehow self-adjusted through the pressure recovery process of the jet from the supply orifices. Thus, a benefit of this injection scheme when applied to the combustor is that predictions of the penetration and mixing performances may be easier because of their insensitivity to the backpressure. Again, the decay of the maximum fraction was insensitive to the injection pressure, with these variations very close to those in the case with the circular, sonic injections.

IV. Conclusions

The matched pressure injections through the diamond-shaped injectors were applied to a Mach 2.5 supersonic crossflow, and the penetration and mixing characteristics of the injected plume were

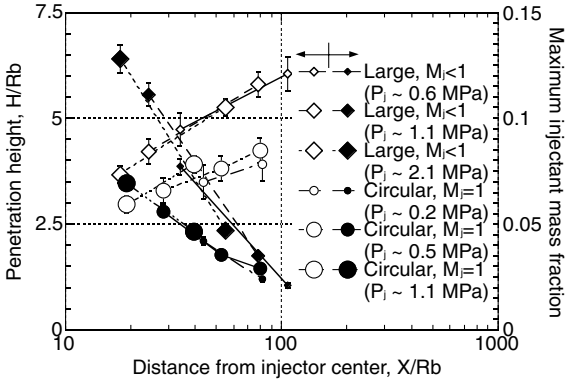

Fig. 10 Summary of penetration and mixing with subsonic injection at various injection pressure.

experimentally investigated. The characteristics of both subsonic and supersonic injections were investigated at the various injection pressure conditions, and were compared to those of the sonic injection to show the following:

1) The matched pressure injection resulted in a less intensive interaction with the freestream, that is, a smaller boundary layer separation ahead of the jet and a less complicated wake flow pattern implying less intensive streamwise vortices generation. However, penalty on the penetration height growth due to the less intensive streamwise vortices generation was not definitive in the present conditions.

2) With the supersonic injection, the plume floated from the injection wall, and the best penetration height was attained over the sonic and subsonic injections. The penetration height was superior to that of the circular supersonic injection, while the benefit of the supersonic injection over the sonic injection at matched pressure conditions was inferior to that in the case with the circular injector. The penetration height increased at the overexpanded condition, while the maximum injectant mass fraction decay was insensitive to the injection condition. This feature is beneficial for applying this injection configuration to supersonic combustors in which a drastic increase in pressure due to heat release is expected.

3) In the case with the subsonic injection, the plume shape was similar to a pillar, and a certain fraction of the injectant was left within the boundary layer region. The penetration height as well as the maximum injectant mass fraction decay was found to be insensitive to the injection pressure.

References

[1] Northam, G. B., Greenberg, I., Byington, C. S., and Capriotti, D. P., "Evaluation of Parallel Injector Configurations for Mach 2 Combustion," *Journal of Propulsion and Power*, Vol. 8, No. 2, 1992, pp. 491–499.

[2] Barber, M. J., Schetz, J. A., and Roe, L. A., "Perpendicular, Sonic Helium Injection Through a Wedge-Shaped Orifice into Supersonic Flow," *Journal of Propulsion and Power*, Vol. 13, No. 2, 1997, pp. 257–263.

[3] Tomioka, S., Jacobsen, L. S., and Schetz, J. A., "Sonic Injection from Diamond-Shaped Orifices into a Supersonic Crossflow," *Journal of Propulsion and Power*, Vol. 19, No. 1, 2003, pp. 104–114.

[4] Cohen, L. S., Coulter, L. J., and Egan, W. J., Jr., "Penetration and Mixing of Multiple Gas Jets Subjected to a Cross Flow," *AIAA Journal*, Vol. 9, No. 4, 1971, pp. 718–724.

[5] Bowersox, R., Fan, H., and Lee, D., "Sonic Injection into a Mach 5.0 Freestream Through Diamond Orifices," *Journal of Propulsion and Power*, Vol. 20, No. 2, 2004, pp. 280–287. doi:10.2514/1.9254

[6] Srinivasan, R., and Bowersox, R., "Simulation of Transverse Gaseous Injection Through Diamond Ports into Supersonic Freestream," *Journal of Propulsion and Power*, Vol. 23, No. 4, 2007, pp. 772–782. doi:10.2514/1.18405

[7] Schetz, J. A., "Interaction Shock Shape for Transverse Injection in Supersonic Flow," *Journal of Spacecraft and Rockets*, Vol. 7, No. 2, 1970, pp. 143–149.

[8] Billig, F. S., Orth, R. C., and Lasky, M., "A Unified Analysis of Gaseous

Jet Penetration," *AIAA Journal*, Vol. 9, No. 6, 1971, pp. 1048–1058.
[9] Kouchi, T., Sakuranaka, N., Izumikawa, M., and Tomioka, S., "Pulsed Transverse Injection Applied to a Supersonic Flow," AIAA Paper 2007-5405, July 2007.
[10] Schetz, J. A., and Billig, F. S., "Penetration of Gaseous Jets Injected into a Supersonic Stream," *Journal of Spacecraft and Rockets*, Vol. 3, No. 11, 1966, pp. 1658–1665.
[11] Orth, R. C., and Funk, J. A., "An Experimental and Comparative Study of Jet Penetration in Supersonic Flow," *Journal of Spacecraft and Rockets*, Vol. 4, No. 9, 1967, pp. 1236–1242.

R. Bowersox
Associate Editor